ISSN 0742-0463, Journal of Volcanology and Seismology, 2016, Vol. 10, No. 2, pp. 100–116. © Pleiades Publishing, Ltd., 2016.
Original Russian Text © E.N. Grib, V.L. Leonov, S.A. Rylova, T.M. Filosofova, A.N. Rogozin, E.S. Klyapitskii, 2016, published in Vulkanologiya i Seismologiya, 2016, No. 2, pp. 32–48.

Melt Inclusions in Quartz Phenocrysts: The Acid Rocks of the Bannaya–Karymshina Area, Kamchatka

E. N. Grib, V. L. Leonov, S. A. Rylova, T. M. Filosofova, A. N. Rogozin, and E. S. Klyapitskii

Institute of Volcanology and Seismology, Far East Branch, Russian Academy of Sciences, Petropavlovsk-Kamchatskii, bul'var Piipa 9, 683006 Russia

e-mail: gen@kscnet.ru

Received April 20, 2015

Abstract—The Bannaya–Karymshina area is situated in southern Kamchatka west of the East Kamchatka Volcanic Belt in the backarc part of the Kuril–Kamchatka island arc. The area is unique in that it contains abundant ejecta of calc-alkaline, acid, mostly ignimbrite, volcanism for a period of 4 Ma. Three rock complexes can be identified with rhyolitic and rhyodacitic compositions: Middle Pliocene ignimbrites, crystalloclastic tuffs of Eopleistocene age that fill in the Karymshina caldera, and Early Pleistocene intrusions. All of these are composed of rocks with normal total alkalinity, while the concentration of potassium places them at the boundary between moderate and high-potassium rocks. We sought to determine the composition of primary acid melts by studying the composition of the silicate phase in homogeneous melt inclusions that were conserved in quartz phenocrysts hosted by volcanic rocks of varying ages. Practically all the melt inclusions we analyzed show increased total alkalies and are in the class of trachyrhyodacites and trachyrhyolites, with the varieties of the highest alkali content being alkaline rhyolites and comendites; the concentration of K_2O classifies them as subalkaline rocks; one also notes the increased alumina of the acid melts. The compositions and spatial locations of the melt inclusions in quartz phenocrysts provide evidence of a three-phase crystallization in magma chambers at different depths. According to the experimental data, the quartz phenocrysts crystallized in a water-saturated melt at pressures of 0.1 to 3.5 kbars.

DOI: 10.1134/S0742046316020044

INTRODUCTION

The Bannaya–Karymshina area is situated in southern Kamchatka west of the East Kamchatka Volcanic Belt in the backarc zone of the Kuril–Kamchatka island arc. Its distance to the trench axis is approximately 300 km and the depth to the Benioff zone is 140–150 km. The nearest larger volcanoes are Gorelyi and Vilyuchinskii, which stand southeast of the area of study. Structurally, the area is confined to the junction between the Nachiki fold–block zone that strikes northwest and the Kambal'nyi–Gorelyi graben. The boundary between these features is the so-called "Vilyuchinskii lineament," which is a major zone of northwest striking discontinuities that traverses all of southern Kamchatka. One unique feature that is peculiar to the Bannaya–Karymshina area consists in abundant ejecta of calc-alkaline, acid, mostly ignimbrite, volcanism for a period of approximately 3–4 Ma (Leonov and Rogozin, 2007; Leonov et al., 2012, 2013). Judging from the volumes of discharged material, this volcanism is comparable with the occurrences of Cretaceous acid volcanism in the Sea-of-Okhotsk–Chukchi Volcanic Belt, which originated in the margin of the North Asian continent. Some researchers believe (Anikin and Miller, 2011) that these geological features are links of a common chain. We inspected the northwestern sector of the Pacific ring to identify several circum-Pacific volcanoplutonic belts of varying ages and suprasubduction origins, beginning from the Late Jurassic–Cretaceous belt, which we believe belongs to the Sea-of-Okhotsk–Chukchi belt. The others are the Campanian–Paleocene belt, which is thought to belong to the Anadyr'–Bristol belt, the Eomiocene belt, which we believe belongs to the Kamchatka–Koryak belt, the Oligocene–Miocene belt, which we believe belongs to the Sredinnyi Kamchatka belt, and the Pliocene–Holocene belt, which we believe belongs to the Kuril–Kamchatka belt; this also includes the Bannaya–Karymshina area. Although all these belts partially overlap, each of them is situated in a comparatively independent area of the continental circumference adjacent to Northeast Asia, with the belt age having the tendency of decreasing toward the Pacific Ocean.

Beginning from the Early Pliocene until the Early Pleistocene, the area of study experienced three phases of calc-alkaline rhyolitic volcanism, which are separated by considerable periods of repose and by the

formation of volcanogenic rock sequences, which differ significantly as to their pyroclastic and lava compositions (Fig. 1) (Leonov and Rogozin, 2007; Leonov et al., 2012, 2013). The oldest phase is represented by Complex I, which consists of dacite, rhyolite, and rhyodacite lavas, tuffs, tuff breccias, and ignimbrites. These show bimodal distributions: dacitic andesites and dacites (62.3–65.1 wt % SiO_2) and rhyodacites (71.1–72.34 wt % SiO_2) are found in the sections of volcanic rocks that make up the basement of the Karymshina caldera. Their age is estimated by the ^{40}Ar–^{39}Ar method to be 3.3–4.01 Ma (the Middle Pliocene). The ignimbrites that were produced during this phase are exposed in the upper reaches of Nachikinskii Brook and around Mt. Sychugan. The next phase of rhyolite volcanism is represented by Complex II, which consists of ignimbrites that are directly related to the Karymshina caldera. Their composition varies from andesites to rhyolites (60.371–74.52 wt % SiO_2). Their age is Eopleistocene (1.7–1.2 Ma) and their area of occurrence is confined to the upper reaches of the Karymchina, Karymshina, Bannaya, and Levaya Bystraya rivers. The caldera is 15 by 25 km and is filled with crystalloclastic tuffs and ignimbrites with a total thickness of 1000 m and a volume of 825 km^3 (Leonov and Rogozin, 2007). This allows us to treat the Karymshina caldera as the largest that is thus far known in Kamchatka and to classify it as a supervolcano (Mason et al., 2004). The youngest phase of acid volcanism in the area is represented by rhyolite extrusions that were emplaced during the post-caldera phase (Complex III); the extrusions are confined to the ring fault that bounds the Karymshina caldera. The extrusions are 0.8–0.5 Ma old. The lavas consist of rhyodacites and rhyolites (70.6–77.4 wt % SiO_2).

The goal of the present paper is to study the compositions of the melts that were involved in generating the acid volcanic rocks of the Bannaya–Karymshina area during several different periods of its history. To do this we studied the melt inclusions (MI) that were conserved during the crystallization of quartz phenocrysts in rhyolites and rhyodacites in the three rock complexes.

The study of inclusions in minerals provides reliable information to judge the composition of the mineral-generating material and the conditions of melt crystallization in volcanic chambers and conduits before the melts arrived to the places of their crystallization (Bakumenko et al., 1976; Ermakov and Dolgov, 1979; Naumov et al., 2008). The study of the compositions of captured crystalline phases provides evidence of an earlier intratelluric phase in the evolution of the magmatic system.

METHOD OF STUDY

Crushed ignimbrites and lavas sampled from the rhyolite and rhyodacite extrusions were inspected under a binocular to identify quartz phenocrysts. These were then converted to polished plates 0.3 mm thick for a study of the distribution and type of the melt inclusions (MI).

The compositions of glasses and crystalline phases were obtained using a Camebax X-ray spectral microprobe at the Institute of Volcanology and Seismology. The inclusions were studied at an accelerating voltage of 15 kV and a current of 30 nA. The analysis of vacuole content was carried out concurrently with an analysis of the host quartz composition in order to provide controls on the analysis accuracy and matrix capture that takes place during the analysis of thin crystalline phases. The MI glass was analyzed point by point and over the available area (using a scanning device) in order to provide controls on possible losses of alkalies. The phases were analyzed at several points. The standards were those in international use, viz., naturally occurring minerals and artificial homogeneous glasses with exact concentrations of individual elements. The analysis was accurate to within 1.5–2%. A total of 84 melt inclusions were studied, of which 20 consisted of two phases (glass + gas) and 8 were composite, with the others being partially crystallized to varying degrees.

A DESCRIPTION OF THE ROCK SAMPLES

Our study of compositions for the basic ignimbrite-generating melts in the Bannaya–Karymshina area drew on samples of the earliest ignimbrites (samples 77-06L and 81-06L) from a section in the upper reaches of Nachikinskii Brook and on samples of the crystalloclastic tuffs that were related to the generation of the Karymshina caldera that filled it during the collapse (samples 48-07L, the middle reaches of the Karymshina river and 140-05L, the western slope of Mount Tolstyi Mys) (see Fig. 1, Table 1). The composition of the acid melts that were involved in the generation of the extrusions was studied using lava samples from extrusive domes and associated flows that are confined to the ring fault that bounds the Karymshina caldera (sample 45-04L, Mt. 1063 m, western side of the feature, samples 112-06L and 114-06L, Mt. 1439 m, southwestern side, sample 63-05L, Mt. 1126 m, north side, sample 105-08L, southwestern side of the feature). Below we provide a description of the rocks.

The Nachikinskii Brook ignimbrites are grey, with a reddish-brown hue, crystallovitroclastic rocks of massive structure. The groundmass, mostly polished sections, shows small fiamme-like glass separations. The crystalloclasts (phenocrysts and their fragments) consist of plagioclase, quartz, sanidine, biotite, titano-

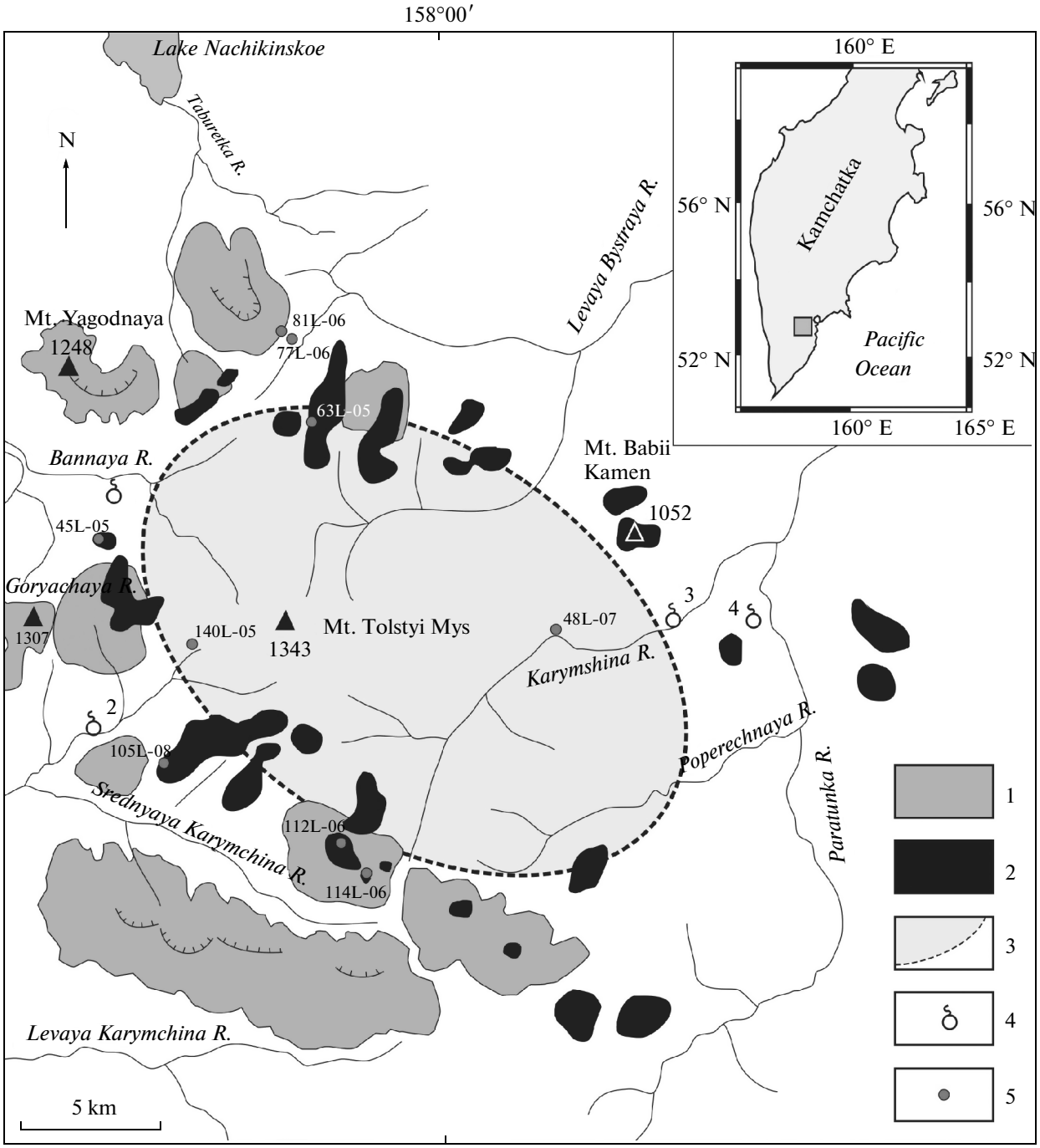

Fig. 1. A map of the Bannaya–Karymshina area.
(1) pre-caldera volcanoes; (2) post-caldera extrusions and lava flows; (3) boundary of the caldera filled with pyroclastic deposits; (4) thermal springs (1, Bol'she–Bannaya; 2, Karymchina; 3, Karymshina; 4, Verkhne-Paratunska). Numerals mark the sampling sites.

magnetite, and ilmenite. Their amounts vary within 25–50% of the rock volume. The sizes vary between 0.05 mm and 0.5 mm, more rarely in the 1.5–2.5-mm range. The plagioclase composition varies from andesine $An_{37–54}$ to sodium oligoclase $An_{18–19}$ (Table 2). The dominant species is poorly zonal phenocrysts of calcium oligoclase $An_{20–27}$. Andesine is encountered in the form of corroded cores in zonal crystals, more rarely nonzonal ones. Potassium feldspar consists of sanidine of a rather constant composition ($Ab_{25–28}Or_{71–77}$), calcium is present in negligible amounts (0.11–0.17 wt %); one occasionally encounters zonal crystals. Zonality is

Table 1. The chemical compositions of samples of acid volcanic rocks in the Bannaya–Kahina area, wt %

Sample #	SiO_2	TiO_2	Al_2O_3	FeO	MnO	MgO	CaO	Na_2O	K_2O	Total
Ignimbrites along Nachikinskii Brook										
77-06L	71.15	0.32	14.22	2.88	0.08	0.87	1.73	3.63	3.62	100.34
Karymshina caldera ignimbrites										
48-07L	72.0	0.28	14.20	3.36	0.09	0.92	2.45	3.79	1.94	99.96
140-05L	70.29	0.32	14.75	2.54	0.08	0.74	2.34	4.13	3.15	101.78
Post-caldera extrusions										
45-05L	73.01	0.24	12.74	1.77	0.08	0.32	1.95	4.44	3.81	100.32
63-05L	75.60	0.23	13.20	1.07	0.07	0.38	1.48	4.04	3.36	99.97
112-06L	76.98	0.15	12.40	1.15	0.07	0.34	0.87	3.70	3.70	99.87
114-06L	76.30	0.15	12.80	0.86	0.07	0.28	0.96	4.00	3.71	99.96
105-08L	74.70	0.17	12.90	1.70	0.08	0.33	1.08	4.05	3.65	100.74

determined by the concentrations of potassium and barium. The concentration of BaO in the sanidine is 1.33–1.5 wt %. The biotite is in phenocrysts and laths with an iron content (fm) of 44–46. The groundmass contains microcrystals (30–40 μm) of chlorine–fluorine apatite and zircon. The apatite contains 1.4–1.6 wt % Cl and 4–6.5 wt % F. Such high concentrations of fluorine typically occur in apatites in the backarc zones of island arcs (Churikova et al., 2004), which is exactly the kind of feature that the Bannaya–Karymshina area is. The groundmass glass consists of high-silica, high-potassium rhyolite of normal alkalinity (77.5–78.79% SiO_2, 4.63–5.52% K_2O, 2.91–3.63% Na_2O), the Na_2O/K_2O ratio is 0.48–0.63.

The Karymshina caldera ignimbrites are typical crystallolithoclastic tuffs of a high degree of baking with a nevadite texture that is due to a large accumulation of crystalloclastic material (up to 55% of the rock volume). The groundmass texture is cinereous and pseudofluidal. The lithoclastic fragments make up no more than 5–10 vol %. The ignimbrites vary in color from grey with brown hues to dark grey. The phenocrysts and their fragments consist of plagioclase, quartz, biotite, titanomagnetite, and ilmenite. Unlike older ignimbrites they do not contain any sanidine. The phenocrysts are dominated by plagioclase of the composition oligoclase $An_{19–27}$. Partially fused, cracked cores in zonal crystals are composed of andesine labradorite $An_{50–55}$, occasionally of bytownite $An_{70–76}$. Plagioclase was found to contain solid-phase inclusions that consist of magnetite, titanomagnetite, ilmenite, chlorine apatite, and biotite. The biotite has an iron content (fm) of 38–42. The titanomagnetite phenocrysts contain 4.2–4.6 wt % TiO_2, with 42–44 wt % in ilmenite.

Extrusive formations. Among these one can identify bodies whose rocks contain sanidine phenocrysts (samples 114-06L, 63-05L, and 105-08L) and those that do not contain them. The latter include rhyolites in the Yashchik extrusion (Mt. 1063 m, sample 45-04L), which lies above the Bol'she-Bannaya thermal springs and in Mt. 1439 (sample 112-06L). The sanidine-bearing rhyolites typically contain plagioclase of the composition oligoclase $An_{15–20}$. The cores in rare zonal crystals are composed of andesine $An_{32–36}$, more rarely of andesine labradorite $An_{52–60}$. The sanidine phenocrysts are mostly zonal, occasionally with resorbed cores. The composition varies in the range $Ab_{31–42}Or_{55–69}$. Calcium occurs in negligible amounts. The high-potassium sanidine makes narrow intermediate or central zones of crystals. Zonality is occasionally of oscillatory character. The concentration of BaO in sanidine varies within 0–3.57 wt %. The patterns that govern the concentration of barium are rather ambiguous; however, a sanidine phenocryst with an oscillatory zonality was found to have its concentration increase in zones of lower concentrations of K_2O. The rhyolite with no sanidine phenocrysts (the Yashchik extrusion) has a plagioclase of greater basicity that consists of poorly zonal calcium oligoclase $An_{24–28}$. The biotite phenocrysts in rhyolite have an iron content (fm) equal to 41–46, with the concentration of TiO_2 in these varying within 3.7–4.5. The sanidine-bearing varieties contain biotite that has a greater iron content (fm = 43–45).

PHENOCRYST TYPE AND COMPOSITION

Two quartz phenocryst types can be distinguished. The one includes comparatively large crystals (0.8–1.5 mm) and fragments of these, which are usually cracked, crushed, and have partially fused, corroded outlines

Table 2. The compositions of glasses in melt inclusions contained in quartz phenocrysts and groundmass glasses in acid rocks, the Bannaya–Karymshina area, wt %

Sample #	SiO_2	TiO_2	Al_2O_3	FeO	CaO	Na_2O	K_2O	Total
Middle Pliocene ignimbrites								
77-06L	71.33		14.83	0.65	0.51	4.76	5.96	98.04
	72.83		13.93	0.41	0.48	5.42	5.45	98.52
	72.4		13.72	0.5	0.57	3.38	5.32	95.89
	73.34		13.43	0.4	0.51	3.13	5.16	95.97
	72.54		14.42	0.63	0.38	5.05	5.6	98.62
	71.77		14.1	0.61	0.37	4.17	5.41	96.43
	71.64		14.9	0.52	0.39	4.3	5.78	97.53
	72.21		14.51	0.48	0.41	4.11	5.86	97.58
	71.73		14.47	0.52	0.38	4.08	5.77	96.95
	71.79		14.48	0.44	0.38	4.13	5.89	97.11
	71.27		15.15	0.6	0.51	4.27	5.94	97.74
	70.9		14.99	0.45	0.43	4.27	5.96	97.00
	71.29		15.57	0.64	0.56	4.1	6.03	98.19
	71.54		15.24	0.56	0.61	4.01	6.08	98.04
	70.85		15.3	0.52	0.64	4.17	6.07	97.55
	71.34		15.07	0.67	0.67	4.06	6	97.81
	70.89		15.21	0.54	0.71	4.26	5.93	97.54
	71.13		15.31	0.66	0.58	4.07	6.02	97.77
	72.29		14.78	0.6	0.63	4.61	5.72	98.63
	70.86		15.3	0.5	0.68	4.04	5.94	97.32
	71.29		13.97	0.55	0.39	4.82	5.51	96.53
	71.01		13.74	0.51	0.35	4.74	5.63	95.98
	71.26		13.72	0.53	0.41	3.95	5.55	95.42
	71.83		14.1	0.5	0.48	4.03	5.59	96.53
	72.85		13.91	0.45	0.35	4.02	5.66	97.24
	72.75		13.9	0.43	0.5	4.97	5.46	98.01
	71.27		14.24	0.41	0.48	4.12	5.61	96.13
	71.65		14.6	0.35	0.45	4.18	5.67	96.90
	71.01		14.66	0.44	0.5	4.24	5.66	96.51
81-06L	70.96		15.1	0.64	0.7	5.01	6.06	98.47
Eopliocene ignimbrites								
48-07L	72.66		15.83	0.62	0.61	4.38	5.68	99.78
	73		15.55	0.55	0.7	4.21	5.62	99.63
Pleistocene extrusions								
45-04L	71.25		15.95	0.10	0.27	4.71	5.35	97.63
	70.91		15.89	0.12	0.33	4.69	5.23	97.17
	77.37		12.65	0.14	0.34	4.51	4.15	99.16
	69.42		16.14	0.13	0.48	4.68	5.83	96.68
	72.25	0.22	15.65	0.15	0.49	4.68	5.46	98.90
	69.70		16.36	0.18	0.30	3.66	5.92	96.12
	69.97		16.27	0.21	0.34	3.86	5.82	96.47
	75.84		12.62	0.18	0.35	3.18	4.98	97.15
	75.36	0.27	13.03	0.28	0.90	3.30	4.51	97.65
	76.19		12.74	0.35	0.45	3.29	4.85	97.87
	76.27		12.70	0.21	0.44	3.05	4.83	97.50
	75.79		12.63	0.33	0.43	3.33	4.84	97.35
	75.09		12.51	0.27	0.45	3.78	4.94	97.04

Table 2. (Contd.)

Sample #	SiO_2	TiO_2	Al_2O_3	FeO	CaO	Na_2O	K_2O	Total
Pleistocene extrusions								
63-05L	74.05		13.97	0.26	0.36	3.80	6.87	99.31
	75.33		13.95	0.1	0.2	3.82	6.25	99.65
	73.16	0.26	16.32	0.59	0.74	3.45	6.24	100.76
	73.82	0.22	16.34	0.7	0.76	3.63	6.22	101.69
	73.2		16.11	0.67	0.67	2.97	6.14	99.76
	76.04	0.25	14.84	0.7	0.78	3.35	5.48	101.44
	72.99		16.13	0.6	0.83	3.51	6.02	100.08
	73.58		15.98	0.61	0.68	2.98	5.98	99.81
	72.41	0.23	16.02	0.64	0.79	3.60	6.10	99.79
	73		16.53	0.79	0.82	3.60	6.10	100.84
	72.25	0.22	16.4	0.73	0.89	3.61	5.98	100.08
	72.66		16.71	0.71	0.86	3.49	6.10	100.53
114-06L	75.8		13.2	0.46	0.26	4.36	5.44	99.52
105-08L	72.15		15.13	0.57	0.58	2.84	6.04	97.31
	78.42		12.73	0.24	0.35	5.56	4.37	101.67
	76.61		12.24	0.62	1.03	4.75	2.99	98.24
112-06L	73.33		14.79	0.58	0.44	3.55	5.52	98.21
	73.25		14.91	0.52	0.49	3.50	5.39	98.06
	73.71		14.86	0.52	0.51	3.42	5.52	98.54
	73.9		14.83	0.53	0.46	4.25	5.61	99.58
	73.43		14.76	0.46	0.57	4.10	5.51	98.83
	74.29		14.7	0.44	0.6	3.72	4.96	98.71
	72.92		15.67	0.62	0.56	3.90	5.44	99.11
	73.64		15.37	0.5	0.48	3.70	5.61	99.30
	73.52		15.21	0.67	0.48	3.61	5.47	98.96
	73.76		15.34	0.57	0.57	4.31	5.42	99.97
Glass in the groundmass of extrusion rhyolite								
114-06L	78.83		12.38	0.42	0.09	1.62	5.66	98.97
	76.82		12.07	0.52	0.25	1.42	5.41	96.59
	78.32		12.41	0.35	0.1	1.44	5.54	98.16
	76.30		12.42	0.38	0.31	1.50	5.23	96.14
112-06L	77.67		12.59	0.23	0.17	1.89	6.13	98.68
	77.45		12.16	0.55	0.32	2.58	5.13	98.36
45-04L	76.11		12.62	0.06	0.67	2.22	4.88	96.56
	76.06		12.25	0.05	0.64	1.93	4.94	95.87
	74.76		12.16	0.08	0.64	2.62	5.4	95.4
105-08L	77.25		12.83	0.53	0.23	2.96	5.37	99.16
	76.92		12.54	0.35	0.21	1.82	5.42	97.25
	77.66		12.76	0.44	0.26	1.75	5.29	98.01
	77.13		12.22	0.48	0.28	1.85	5.39	97.35
	77.35		12.16	0.46	0.23	1.68	5.25	97.43
63-05L	77.18		12.78	0.1	0.26	2.39	6.13	98.64
	77.54		12.98	0.11	0.47	2.8	5.93	98.9

with bay-shaped groundmass emplacements, which shows that they were not in equilibrium with the host melt. The corroded phenocrysts make up 5–10% of the rock volume. The other type includes small rounded grains that are practically devoid of inclusions.

The Nachikinskii Brook ignimbrites. Quartz phenocrysts of the first type contain two-phase (uncolored glass + gas), composite, and transformed melt inclusions (MIs) (Ermakov and Dolgov, 1979). Glassy MIs 10–100 μm across are encountered as azonal groups that contain two to four individuals. The vacuoles have isometric shapes, are oval, one occasionally discerns a bipyramidal negative shape of high-temperature quartz (Figs. 2a, 2b). A gas bubble usually occupies 10–15% of the inclusion volume. One occasionally encounters depressurized MIs with pumice-like glass in the region where the gas bubble is situated. Such inclusions are usually surrounded by small cracks in the host quartz, which provide evidence of a high-fluid pressure in the inclusion (during quartz crystallization). The glass in the inclusions has a trachyrhyodacitic composition with increased potassium alkalinity and high alumina (70.23–72.83 wt % SiO_2, 5.72–6.06 wt % K_2O, 4.27–5.01 wt % Na_2O, 14.47–14.94 wt % Al_2O_3, see Table 3), the Na_2O/K_2O ratio is 0.72–0.83, and Cl = 0.11–0.14 wt %. The deficit of the sum of components in MI glass (97.3–98.6 wt %) allows one to estimate the maximum content of dissolved water (1.4–2.6 wt %). Partially crystallized MIs usually have rounded shapes and are 80–130 μm across (see Fig. 2c). The glass is inlaid with thin exhalations of titanomagnetite and ilmenite. The inner part of an inclusion frequently has a druse texture with thin-crystallized phases with the compositions of sanidine cryptoperthite ($Ab_{35}Or_{65}$) and anorthoclase cryptoperthite ($Ab_{80}An_{11}Or_9$) (Table 4). The crystalline filling is crushed, probably during depressurization. The composite MIs have oval shapes and are 50–80 μm with rough boundaries (see Fig. 2d). The phases include adularia (sanidine?) ($Ab_{10-13}Or_{87-90}$) and foamed glass of albite composition ($Ab_{95-99}Or_{1-5}$). Potassium feldspar in turn contains a solid-phase inclusion of manganese clinopyroxene 5 μm across (the composition is intermediate between ferrosillite and hedenbergite, see Deer et al., 1962). The concentration of MnO in the latter varies between 4 and 10.8 wt %. The quartz phenocrysts that were found in ignimbrites along Nachikinskii Brook are mostly transformed MIs. Their sizes vary in the 100–300 μm range. They resulted from corrosion that affected quartz of the first type on the part of the groundmass, penetrating inside the crystals (see Fig. 2a). The shape of the inclusions can be drop-shaped, amoeboid, or worm-like. The inclusions are composed of potassium–sodium zeolite (clinoptilolite) forming sheaf-like and radial aggregates, and of chlorite (penine). The transformed inclusions are occasionally encountered alongside glassy MIs (see Fig. 2a).

The solid-phase inclusions in quartz include biotite in the outer zones of phenocrysts and chlorine–fluorine apatite. When found near biotite, quartz is enriched in Sn, Yb, Hg, Tl, and Np. The ignimbrite groundmass around quartz crystals was found to contain microphenocrysts that consist of sanidine (Ab_{27-31}, Or_{69-77}, Bao = 1.33–1.43%), oligoclase ($Ab_{71-72}An_{21-23}Or_{5-6}$), and more rarely of andesine ($Ab_{53}An_{40}Or_5$).

The intracaldera ignimbrites of the Karymshina caldera. The bulk composition of ignimbrites is consistent with rhyodacite of normal alkalinity. The quartz phenocrysts in these ignimbrites were found to contain only two glassy MIs 20–30 μm across (Fig. 3a). Homogeneous colorless glass has a trachyrhyolitic composition with high concentrations of potassium and alumina (72.66–73.00% SiO_2, 5.62–5.68% K_2O, 4.21–4.38% Na_2O, 15.55–15.83% Al_2O_3); the Na_2O/K_2O ratio is 0.75–0.78, and Cl = 0.13–0.14 wt %. The compositions of these inclusions are close to that of the highest alumina MIs from the older ignimbrites. The quartz phenocrysts in intracaldera ignimbrites are dominated by partially crystallized MIs where the melt is laminated to varying degrees (see Figs. 3b, 3c, 3d). The inclusions vary in size between 50 and 400 μm, the smaller vacuoles (50–100 μm) are oval, the larger ones have amoeboid-like shapes. The larger inclusions are connected to the groundmass, which is apparent in polished sections. The smaller inclusions are encountered in azonal groups and are obviously primary in origin. The vacuole filling is brownish to yellow in color. The lamination is seen as alternating quartz and feldspar clusters. The simplest expression of lamination was recorded in the smaller inclusions (see Fig. 3b). There is a thin (approximately 3 μm) layer of glass in contact with the host quartz, the glass is extremely acid with sodium specialization and low alumina (86.1–90.18% SiO_2, 0.79–1.59% K_2O, 1.49–2.82% Na_2O, 5.79–8.13% Al_2O_3), the Na_2O/K_2O ratio is 1.35–3.5. These are so-called eutaxitic melts that are similar to the host crystal in composition. This is followed by a layer of high-potassium, high-alumina glass of a trachyrhyolitic composition 4–5 μm thick (77.5–78.79% SiO_2, 4.63–5.52% K_2O, 2.91–4.63% Na_2O, 16.87–18.5% Al_2O_3); the Na_2O/K_2O ratio is 0.48–0.63. The middle parts of the inclusions are composed of quartz and quartz glass with fine ore dust. The inclusion is of a primary origin, as shown by small gas cavities around the vacuole. Some of the MIs show a lamination that is seen as alternating glasses of varying silicic acid contents and alkalinities (74.4–88.93% SiO_2, 0.74–9.18% K_2O, 1.22–3.44% Na_2O, 5.53–12.48% Al_2O_3) (see Figs. 3c, 3d). The larger MIs have the concentration

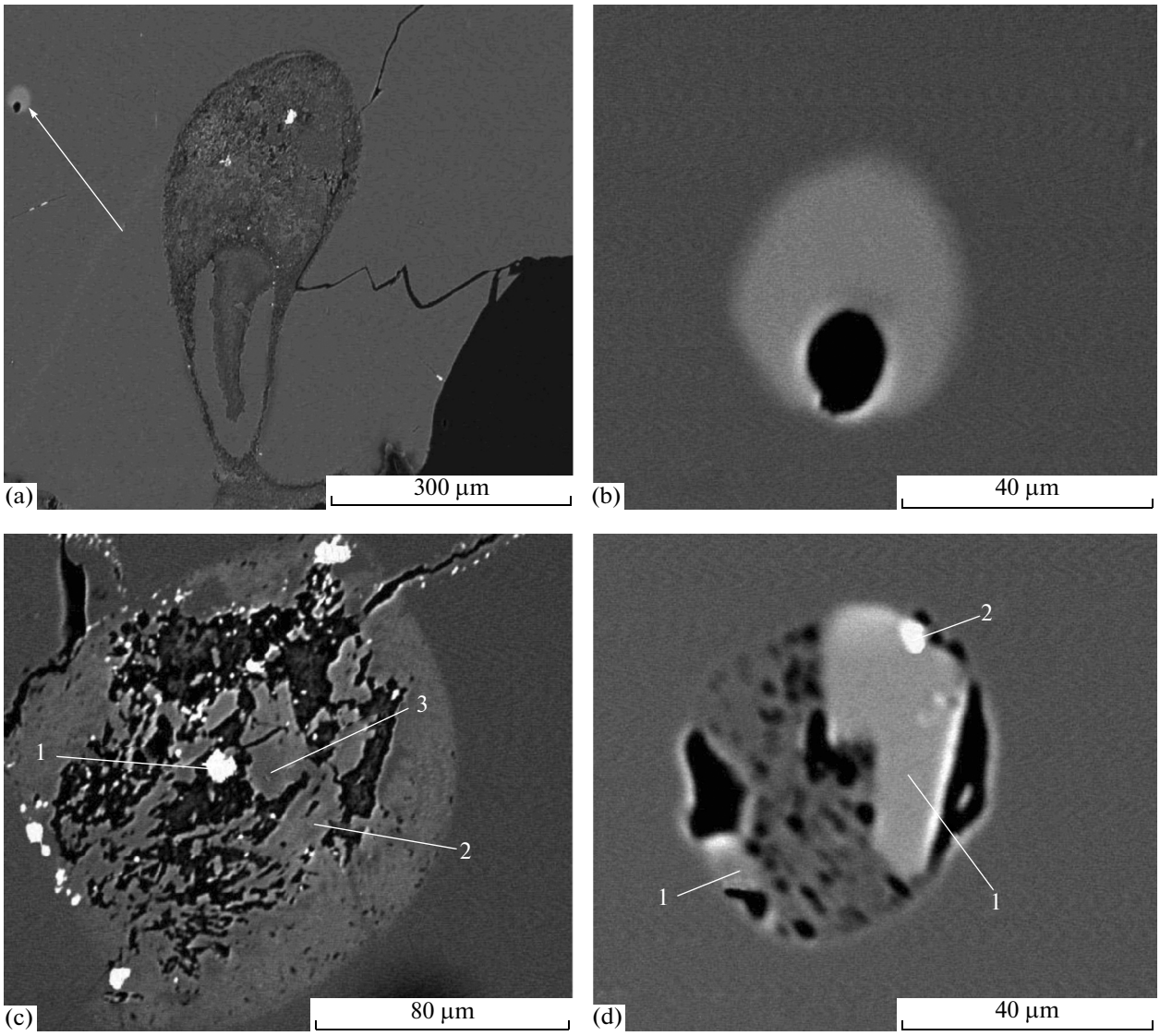

Fig. 2. Melt inclusions in the quartz of Pliocene ignimbrites (Nachikinskii Brook).
(a–c) sample 77-06L: a, a transformed (altered by secondary processes) melt inclusion resulting from corrosion of quartz crystals, a minor glassy MI (marked by an arrow in the upper corner); b, the same glassy MI under a greater magnification; c, partially crystallized MI along the periphery of the margin of high-silica, high-potassium glass with thin veins of quartz glass. The glass is inlaid with fine exhalations of titanomagnetite (1) and of ilmenite. The central part contains fine-crystalline phases of sanidine cryptoperthite (2) and of anorthoclase cryptoperthite (3). The inclusion has been depressurized; d, composite MI with a fine-crystalline phase of adularia (1) (sanidine?) and with a foamed albite glass; adularia (sanidine?) contains a solid-phase inclusion of manganiferous clinopyroxene (hedenbergite) (2), sample 81-06L.

of K_2O increasing in feldspar clusters toward the center, as far as cryptocrystalline sanidine aggregates. The feldspar interbeds are thinner. Small gas cavities occur throughout the entire volume of an MI, with the vacuole content being occasionally broken with settling cracks. MIs with less pronounced lamination also occur, but they invariably contain quartz–feldspar components.

Extrusive formations. The lavas in extrusions are mostly rhyolitic and have normal alkalinity. Quartz phenocrysts vary within the range 0.3–0.6 mm across, but more rarely reach 1 mm. The melt inclusions in these are glassy, partially crystallized, and composite types. The first type includes MIs that consist of pure glass and a gas bubble, more rarely two bubbles (Figs. 4a, 4b). The gas bubble occupies 10–20% of the MI volume. The MIs vary between 40 and 100 μm in size. The inclusion shapes frequently bear the impress of a negative bipyramidal shape that is peculiar to high-temperature quartz. The silicate phase in MIs varies in a wide range (69.42–76.61% SiO_2, 5.23–6.22% K_2O, 3.66–4.71% Na_2O, 15.65–16.36% Al_2O_3). A narrow

Table 3. The compositions of phenocrysts in acid rocks of the Bannaya–Karymshina area, wt %

Phase	SiO_2	TiO_2	Al_2O_3	FeO	MgO	MnO	CaO	Na_2O	K_2O	BaO	Total
	Middle Pliocene ignimbrites										
Pl_c	65.86	0.0	25.52	0.17	0.0	0.0	7.69	6.71	0.48		100.43
Pl_{mg}	61.98	0.0	24.24	0.11	0.0	0.0	5.21	8.17	0.83		100.54
San	63.7	0.0	19.15	0.11	0.0	0.0	0.13	2.69	12.11	1.33	97.9
Bi	37.04	4.54	13.69	17.63	12.11	0.37	0.12	0.51	9.80		98.88
TiMt	0.0	3.88	0.55	94.29	0.01	0.30	0.0	0.0	0.0		99.14
Ilm	0.16	45.72	0.08	41.26	0.333	3.41	0.0	0.0	0.0		95.13
	Eopliocene ignimbrites										
Pl_c	61.62	0.0	24.93	0.23	0.0	0.0	5.99	7.53	0.68		100.98
Pl_{mg}	61.77	0.0	23.71	0.19	0.0	0.0	4.54	8.05	0.86		99.12
Bi	37.58	4.17	14.15	15.46	13.71	0.35	0.0	0.48	9.38		99.23
TiMt	0.0	4.17	0.83	95.2	0.08	0.37	0.0	0.0	0.0		100.68
	Pleistocene extrusions										
Pl_c	64.08	0.0	22.03	0.15	0.0	0.0	3.72	9.37	0.99		100.34
Pl_{mg}	65.08	0.0	22.33	0.16	0.0	0.0	3.48	9.59	0.97		101.61
San_c	64.26	0.0.	19.38	0.10	0.0	0.0	0.12	3.81	11.43	1.07	99.63
San_{mg}	63.4	0.0	19.11	0.03	0.0	0.0	0.11	3.66	11.03	2.99	99.73
Bi	37.06	3.84	14.31	18.02	12.75	0.40	0.0	0.33	9.23		99.91
Gl	76.82	0.11	12.17	0.52	0.05	0.0	0.28	1.42	5.41		96.75

Notations for phenocryst minerals: Pl, plagioclase, San sanidine; Bi, biotite; TiMt, titanomagnetite; Ilm, ilmenite; and Gl, glass. The letter c denotes the phenocryst center and mg the phenocryst margin.

(2–5 μm) margin of high-silica glass with a low potassium concentration (77.37–84.9% SiO_2, 0.32–1.47% K_2O) is occasionally observed in MIs that are in contact with quartz. When it occasionally happens that a single grain contains several glass inclusions of different compositions it is found that low silica but high-alumina and higher alkaline MIs are confined to the inner parts of a phenocryst (see Fig. 4b). Glassy MIs with sodium specialization are unusual. One can see in Fig. 4b that high-sodium glass fills in wedge-like cracks that point into the inner part of the host quartz and is finely foamed in contact with the quartz (76.55–79.06% SiO_2, 0.22–0.32% K_2O, 6.72–7.17% Na_2O, 11.99–12.72% Al_2O_3, the Na_2O/K_2O ratio is 14–21, Cl = 0.22–0.32 wt %). When viewed in cross section, the shape of these inclusions is oval, with no gas bubble. They are obviously of later origin and seem to have formed when the groundmass glass penetrated into the crystal along cracks after the body had been formed. The groundmass glass of host rhyolite is perlitized on cooling and underwent devitrification; the rhyolite also contains thin glass interbeds with sodium prevailing over potassium. The composite MIs (see Figs. 4e, 4f) are characterized by the fact that they captured small crystals (accessories) along with a melt drop. The crystals were separated from the parent melt before the MIs were formed (Bakumenko et al., 1978; Ermakov and Dolgov, 1979). Such solid-phase inclusions consist of sanidine ($Ab_{30–31}Or_{69–70}$), apatite, zircon (74.3 wt % Zr), monazite (13.8 wt % P, 8.55 wt % La, 20.02 wt % Ce, and 6.55 wt % Nd), and manganiferous clinopyroxene (4–10 wt % MnO). The Yashchik lavas (sample 45-04L), which do not contain sanidine among the phenocrysts, have potassium feldspar in MIs defined as an accessory crystal. This feldspar has the composition of adularia (Ab_8Or_{92}) (see Fig. 4e). Since adularia is not a magmatic mineral, it may be supposed that potassium feldspar, possibly sanidine, has been transformed into adularia due to penetrating hydrothermal brine. Partially crystallized MIs are not uniformly distributed in quartz phenocrysts, which occasionally occur in association with glass inclusions of the first type (see Figs. 4c, 4d). They vary in size in the 50—150-μm range. Their shape is oval and irregular. The filling of the MIs consists of inhomogeneous high-silica glass of potassium specialization (74.05–77.32% SiO_2, 4.33–6.87% K_2O, 3.80–5.84% Na_2O, 11.35–14.73 Al_2O_3; the Na_2O/K_2O ratio is 0.57–0.87, Cl = 0.14–0.20 wt %). The centers of the larger specimens contain fine exhalations of sanidine cryptoper-

Table 4. The composition of solid-phase inclusions in MIs from the Bannaya–Karymshina acid rocks

##	Phase	SiO_2	TiO_2	Al_2O_3	FeO	MgO	MnO	CaO	Na_2O	K_2O	Total
	Middle Pliocene ignimbrites										
1	Pl	65.34	0.0	21.20	0.43	0.0	0.0	2.36	9.84	1.58	100.76
2	San1	65.40	0.0	18.05	0.40	0.0	0.0	0.0	3.81	10.99	99.78
3	TiMt	0.0	2.53	2.37	81.63	0.0	0.59	0.0	0.0	0.0	93.69
4	San2	64.99	0.0	18.35	0.0	0.0	0.0	0.0	1.29	16.07	99.93
5	CPx	49.39	1.40	4.52	9.60	3.93	10.81	18.50	0.90	0.53	99.56
6	Gl-Pl	67.99	0.0	18.91	.0	0.0	0.0	0.40	10.85	0.0	98.16
	Eopliocene ignimbrites										
7	San	66.29	0.0	17.29	0.76	0.0	0.0	0.0	1.00	14.40	100.19
8	Ilm	0.18	52.89	2.30	35.84	0.0	0.34	0.32	0.52	0.55	93.33
9	TiMt	0.0	3.92	2.60	84.92	0.0	1.50	0.20	0.0	0.0	93.13
	Pleistocene ignimbrites										
10	Pl	66.77	0.0	19.15	0.65	0.0	0.0	0.92	9.12	3.55	100.17
11	San	65.75	0.0.	17.59	0.30	0.0	0.0	0.0	3.45	11.29	98.38
12	CPx	48.52	0.92	4.98	8.15	7.21	5.60	19.69	2.12	0.16	97.86
13	San	64.44	0.0	18.61	0.0	0.0	0.0	0.0	0.92	15.92	99.89

(1–6) solid-phase inclusions in MIs in the quartz of Middle Pliocene ignimbrites: (1–3) (Fig. 2c): (1) anorthoclase cryptoperthite, (2) sanidine cryptoperthite, (3) titanomagnetite; (4–6) (Fig. 2d): (4) adularia, (5) manganiferous clinopyroxene, (6) albite glass; (7–9) solid-phase inclusions in MIs in the quartz of Eocene to Pliocene ignimbrites: (7) sanidine from feldspar clusters in partially crystallized, laminated MIs, (8–9) fine exhalations of titanomagnetite and ilmenite in these MIs; (10–13) solid-phase inclusions in MIs in the quartz of extrusions: (10–11) (Fig. 4d) anorthoclase (10) and sanidine (11); (12–13) (Fig. 4e) clinopyroxene (12), adularia (13).

thite ($Ab_{31–45}Or_{58–63}$) or of anorthoclase cryptoperthite ($Ab_{42–51}Or_{47–58}$) and quartz. Practically all partially crystallized inclusions have been depressurized and are accompanied by "moustaches" that consist of cracks that branch away from the inclusions.

RESULTS AND DISCUSSION

The information that is stored in melt inclusions. The quartz phenocrysts in the Bannaya–Kamyshina acid rocks contain several different types of melt inclusions: glassy, variously crystallized, transformed, and laminated. All of these supply definite information on the processes that were occurring during different phases in the evolution of melts and rocks; for example, transformed melt inclusions in the quartz of Middle Pliocene ignimbrites reflect the degree of nonequilibrium (corrosion) for individual quartz phenocrysts in the host melt. These resulted from interaction between glass and the hydrothermal solutions that penetrate into inclusions along cracks during the posteruptive period, or else are directly related to the groundmass. Some locations contain cryptocrystalline phases of sanidine and quartz glass. Inclusions of the laminated type, which dominate the quartz phenocrysts of intracaldera ignimbrites, are rather unusual for MIs in acidic effusive and pyroclastic rocks. They can be compared with the "flow lamination" that arises in smaller magma bodies that penetrate a heated material (Sharkov, 2006). In that case the melt does not have to undergo rapid cooling. As the melt cools still more, it reaches a pre-crystallization state and acquires properties of a Newtonian fluid involving the viscoplastic type of flow. The lamination in bodies of this type is peculiar in having the following features: (1) a two-member character of rhythmicity; (2) it is always oriented parallel to the contacts, mimicking their configuration; (3) the interlayer contacts are gradual; (4) the layers in the middle can be deformed to form folds, can be ruptured and isolated. These features in the lamination of minor magma bodies are observed in larger laminated MIs in quartz from the Karymshina caldera ignimbrites. Judging from the fact that the laminated features have been preserved, the solidification was instantaneous. According to (Sharkov, 2006), this type of lamination arises in acid, as well as in basic, melts. The acid melts typically involve quartz–feldspar clusters that act as the structure-forming agent. In the case under consideration, when the emptied apical part of a magma chamber collapsed, the mass of pyroclastic material descended along with the caldera bottom and was in a heated state during some time. It would be difficult to envisage plastic flow in a melt inclusion, but some movements were certain to have occurred in the total mass of this body until its evolution was completed. The groundmass of intracaldera ignimbrites also involves lamination, which is seen as alternating layers with different concentrations of potassium, which is typical of larger melt inclusions.

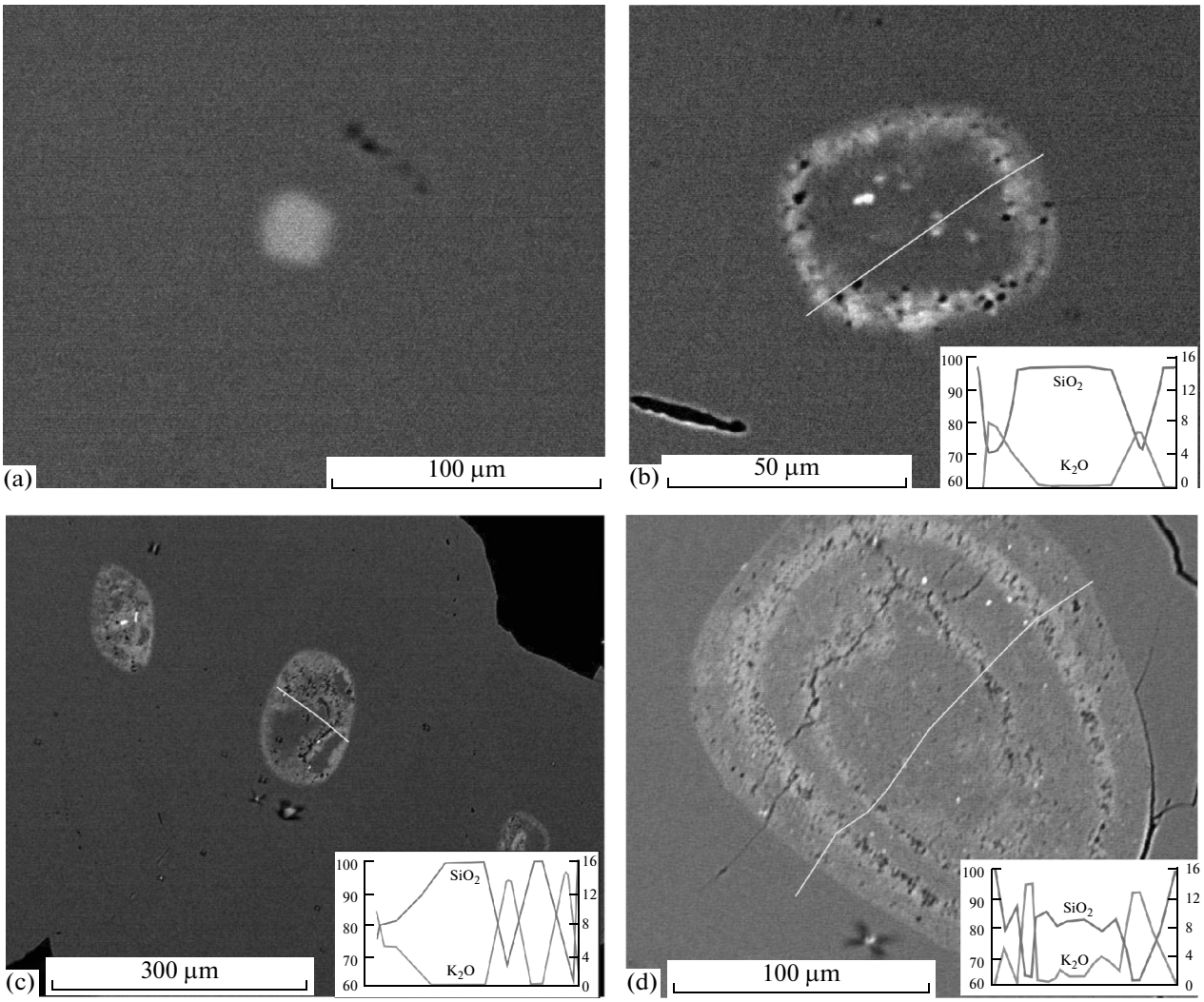

Fig. 3. Melt inclusions in quartz phenocrysts from Eocene–Pleistocene intracaldera ignimbrites with partial crystallization and lamination of the glass.

a, an MI with a low degree of lamination; b, a large MI with a rhythmic lamination; c, a set of laminated MIs. The solid phase consists of sphene and titanomagnetite; d an MI with deformed lamination. The plots show the distributions of SiO_2 and K_2O in inclusions along the lines shown in this figure; a, b, d, sample 140-06L, c 48-06L, b, arrow indicates a small glassy inclusion.

The most information is gathered from homogeneous two-phase inclusions that consist of glass and a gas bubble. These primary MIs in quartz phenocrysts reflect the composition and physico-chemical conditions that existed at depths until the melt came to the ground surface. It was only this type of inclusion that we analyzed in the present study to acquire information on the composition of primary melts. Inclusions did not experience homogenization, since the glasses of individual MIs had uniform compositions. It is only in contact with host quartz that we could occasionally observe a thin (a few μm) margin of a high-silica low-potassium, melt.

The composition of melt inclusions and physico-chemical conditions during the crystallization of acid melts. The Bol'she–Bannaya acid volcanic rocks of different ages are rocks of normal total alkalinity, while the concentration of K_2O places them at the boundary

Fig. 4. Melt inclusions in quartz phenocrysts from Early Pleistocene extrusive features.

a–c, MIs of different types (glassy and slightly crystallized); d, a partially crystallized inclusion: a rim of inhomogeneous high-potassium glass; at the center are solid-phase inclusions of sanidine (1) and of quartz (2); e, a composite MI: accessory microcrystals of analcime (sanidine?) (1) and of manganiferous clinopyroxene (hedenbergite) (2); f, a composite inclusion that consists of an accessory zircon crystal with a captured drop of melt; a, sample 112-06D, b, e, f, sample 45-04, c, sample 105L, d, sample 114-06L. In the inset (b) the arrow points to a small glassy MI.

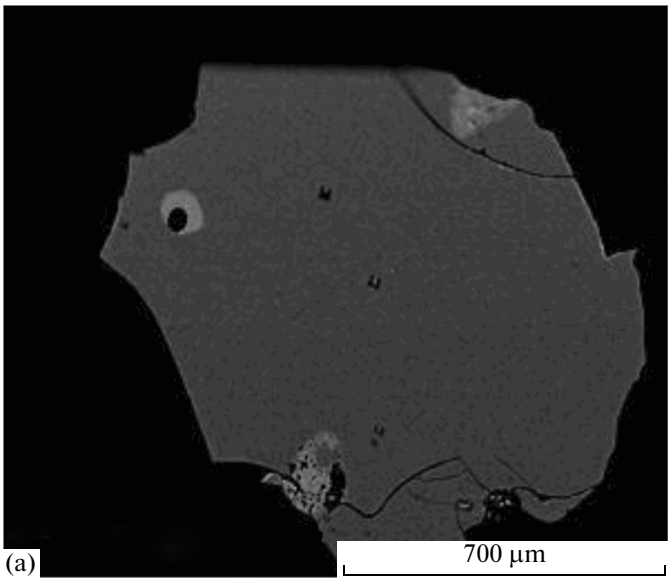
(a)
700 μm

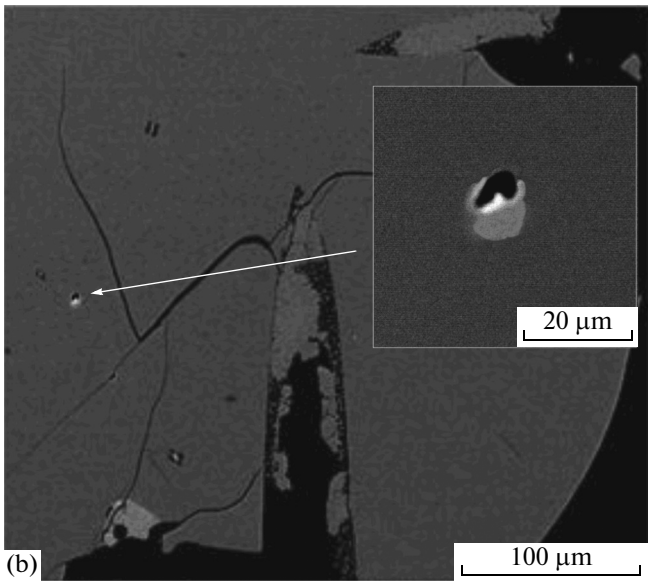
20 μm
(b)
100 μm

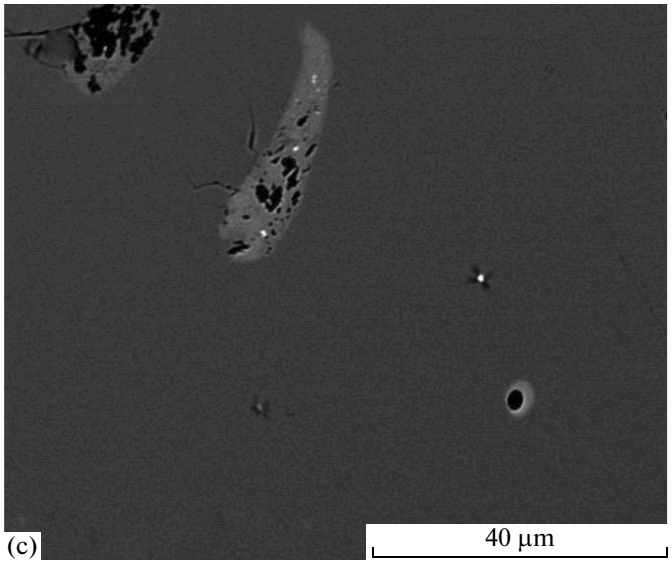
(c)
40 μm

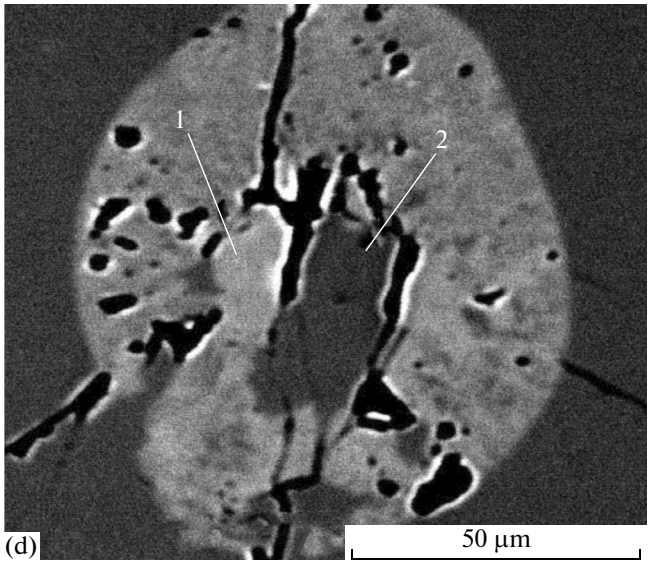
1
2
(d)
50 μm

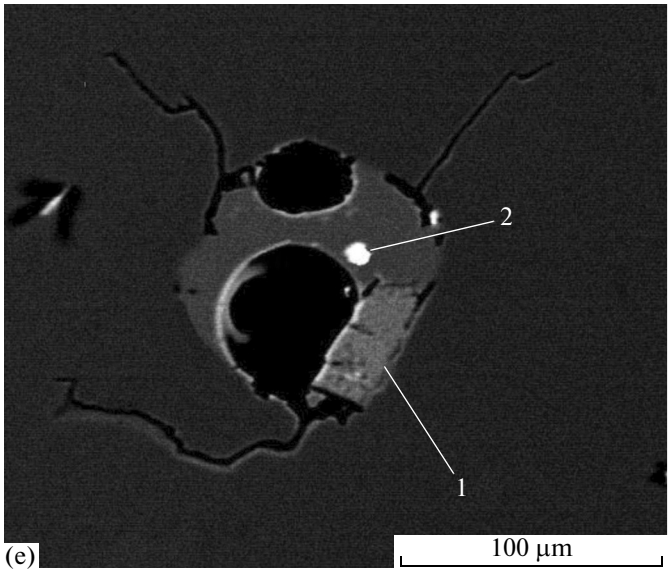
2
1
(e)
100 μm

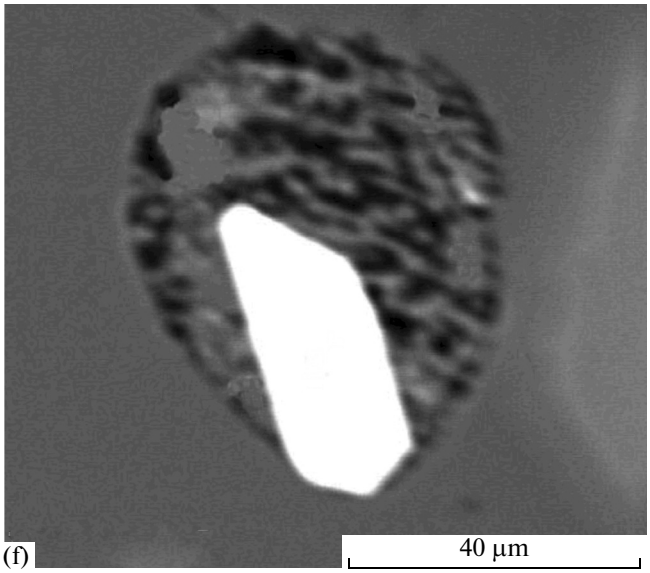
(f)
40 μm

of moderate and high-potassium rocks of the calc-alkaline series (Fig. 5). At the same time, practically all glass MIs in quartz phenocrysts that we have analyzed showed increased potassium concentrations and should be classified as belonging to the subalkaline type.

The composition of glass for homogeneous MIs in quartz phenocrysts from ignimbrites, both older ones along Nachikinskii Brook and the ignimbrites of the Karymshina caldera, varies in the range between 70.86 and 74.34 wt % SiO_2 (see Table 3). With regard to the bulk composition of ignimbrites, they have higher total alkalinity (8.7–11.17 wt %) and are to be classified as trachyrhyodacites according to this criterion, less probably as alkaline rhyodacites, and even comendites. Judging by the concentration of K_2O, they belong to the subalkaline series. They typically show moderate concentrations of FeO (0.22–0.66 wt %) and of CaO (0.35–0.68 wt %). The concentration of TiO_2 in the silicate phase of MIs does not exceed 0.22–0.27 wt % and is close to that in the rocks, but it is not determinable in all inclusions. MgO is not determinable in glass. Judging by the concentration of Al_2O_3 (13.7–15.5 wt %), the glass in the MIs is close to ignimbrites as to bulk composition and has increased concentrations of alumina that are typical of subalkaline rocks. The agpaitic index ($Al_2O_3/CaO + Na_2O + K_2O$) is 1.24–1.56 (*Petrograficheskii kodeks ...,* 2009). It should be noted that the compositions of glass in a few glassy MIs that were found in the quartz of intracaldera ignimbrites have higher silica contents and are close to those of MIs in phenocrysts of post-caldera extrusions.

The silicate phase of MIs in quartz phenocrysts from rhyolites of post-caldera extrusions makes up a wide series of compositions from 69.4 to 78.4 wt %, judging by the concentration of SiO_2 (see Fig. 5, Table 3). Based on this parameter, they can be subdivided into three sets: low silica (69.4–71.0 wt %), moderate silica (72.5–74.1 wt %), and high silica (75–78.4 wt %). The second set is dominant. The set mostly includes MIs in extrusions where sanidine occurs among phenocrysts. These have compositions that are intermediate between trachyrhyodacites and trachyrhyolites, have higher silica (13.97–16.7 wt % Al_2O_3) and higher concentrations of FeO (0.26–0.79 wt %) and of CaO (0.36–0.89 wt %). According to total alkalies they are at the boundary between moderate alkaline and alkaline series, while the concentration of K_2O (5.98–6.87 wt %) classifies them as belonging to the calc-alkaline and subalkaline series. The agpaitic index is 1.38–1.65. According to these parameters they are close to MI glass in ignimbrite quartz, but have higher SiO_2. The first set of trachyrhyodacite inclusions is encountered only in the Yashchik rhyodacites where potassium feldspar has not been detected among phenocrysts (but has been detected as accessory crystals in some of the MIs). According to the concentrations of potassium and alumina they are little different from the MIs in the second set, but have lower concentrations of iron (0.1–0.21 wt %) and of calcium (0.27–0.48 wt %). Lastly, the MIs in the third set have compositions of high-silica trachyrhyolites, show lower alumina concentrations (12.24–13.02 wt %) and lower potassium (4.15–5.1 wt %), varying concentrations of FeO (0.1–0.62 wt %) and of CaO (0.2–0.78 wt %). According to the concentration of potassium they belong to the high-potassium calc-alkaline series. The MIs of the third set are encountered both in lavas that contain sanidine phenocrysts and in lavas that do not. According to the concentrations of the main components (SiO_2, Al_2O_3, FeO, CaO) they are the closest to the glass that is found in the groundmass of extrusion rhyolites (see Fig. 5). The leading differences (the scatter) are in alkalinity and are probably related to devitrification of groundmass glass. The glass of MIs in the samples that we studied contain insignificant (0.1–0.22 wt %) amounts of chlorine, which is characteristic for acid melts. Its highest concentrations (0.18–0.22 wt %) were recorded in MI glass from Yashchik quartz.

The SiO_2 vs. oxide diagram (see Fig. 5) has the compositions of melt inclusions in quartz phenocrysts from pumice tuffs of the Polovinka caldera in the Karymskii Volcanic Center (Naumov et al., 2008). They have compositions of high-silica rhyodacites and low-silica rhyolites, and according to this parameter they are the closest to the MIs of the second set in the quartz of extrusive features. They differ from the Bannaya–Karymshina melt inclusions by the concentrations of leading rock-forming components in having lower total alkalies and lower alumina, which is characteristic for the volcanic rocks of the East Volcanic Belt and in having comparatively higher concentrations of FeO and CaO. The concentration of chlorine in MI glass in quartz from the pumice tuffs of the Polovinka caldera is similar (0.1–0.15 wt %) to that in rhyolitic MIs for the area of study.

Judging from the deficit of the analytical glass sums for the MIs analyzed, the concentration of water in the melt was 1.4–5 wt %. The points of normative MI compositions as plotted in the ternary Ab–Qtz–Or plot for the granite system (Fig. 6) with experimental cotectic curves that correspond to different pressures at higher water concentrations in the melt (Shinkarev, 1970; Ehlers, 1972; Winter, 2001) show a scatter that increases toward the quartz corner and reveal some enrichment in the Or component relative to the normalized bulk composition of the rocks. The latter plot is near the points of the temperature maximum in cotectic curves and also shows an evolution toward the quartz corner. Judging from the locations of anal-

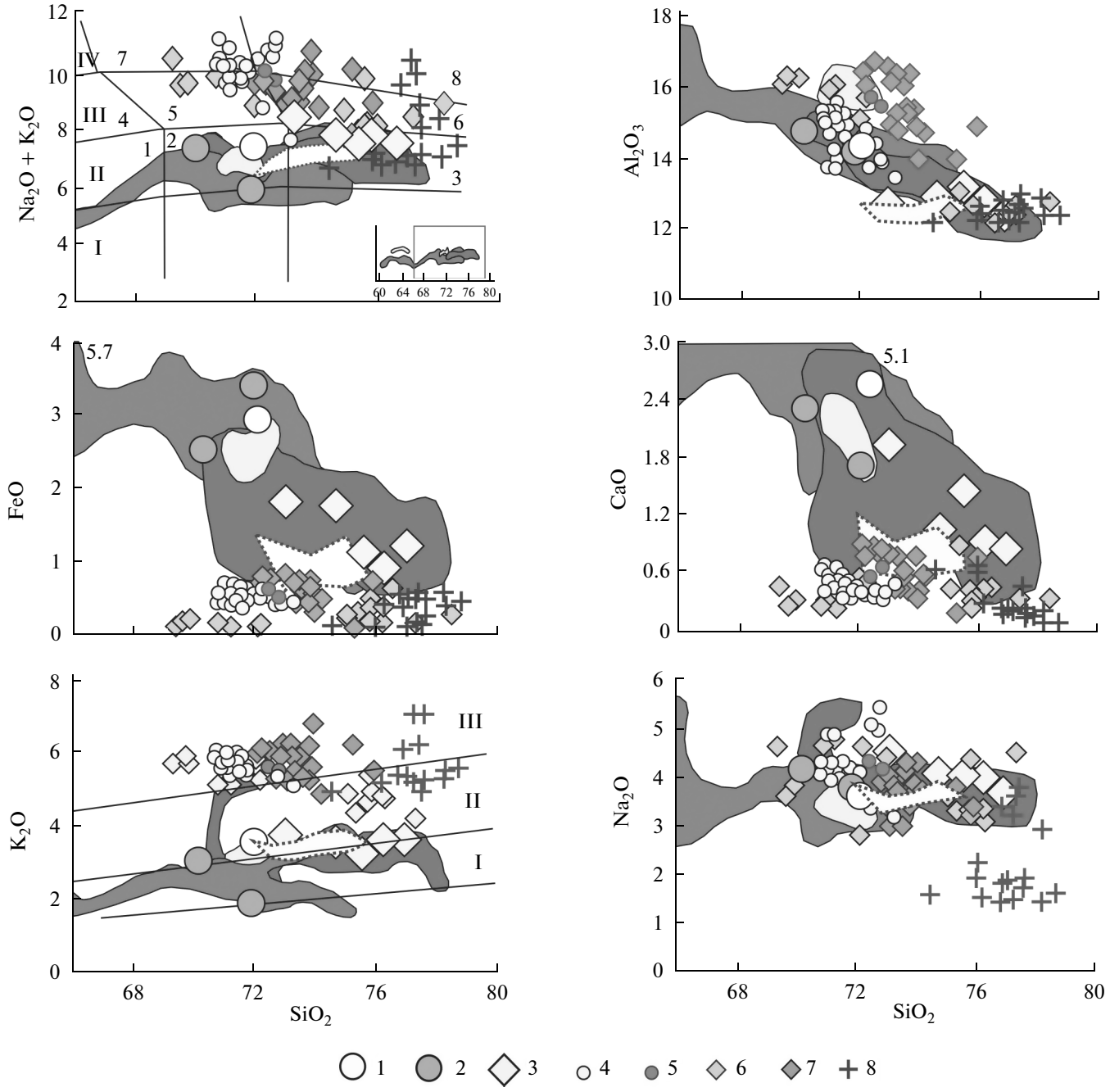

Fig. 5. The MI composition in the Bannaya–Karymshina acid rocks plotted in the SiO_2–oxides coordinates, wt %.

Bulk compositions: (1) Pliocene ignimbrites, Nachikinskii Brook, (2) intracaldera ignimbrites, (3) post-caldera extrusions; (4–7) compositions of melt inclusions in quartz: (4) in Pliocene ignimbrites, (5) in intracaldera ignimbrites, (6) in postcaldera extrusions that contain sanidine in their phenocrysts, (7) in the quartz of the postcaldera Yashchik extrusion, sample 45-04, whose phenocrysts do not contain sanidine, (8) compositions of groundmass glasses; composition fields for quartz-bearing acid rocks: white (boundary marked by dotted line) denotes compositions of melt inclusions in quartz phenocrysts sampled from pumice tuffs of the Polovinka caldera, Karymskii Volcanic Center; lighter grey denotes Pliocene ignimbrites, grey marks intracaldera ignimbrites, and darker grey the postcaldera extrusions. Numerals in the classification diagrams denote fields of the following rock series: $Na_2O + K_2O$ low alkaline (I), normal alkaline (II), moderate alkaline (III), alkaline (IV); K_2O moderate potassium, calc-alkaline (I), high-potassium, calc-alkaline (II), and subalkaline (III) (Peccerillo and Taylor, 1976). The numerals in the $Na_2O + K_2O$ diagram indicate the fields of different rock types according to (*Petrograficheskii kodeks ...*, 2009): (1) dacites, (2) rhyodacites, (3) rhyolites, (4) trachydacites, (5) trachyrhyodacites, (6) trachyrhyolites, (7) alkaline rhyodacites, (8) comendites. The numerals in the FeO and CaO diagrams indicate the extreme concentrations in precaldera and intracaldera ignimbrites. The oxide concentrations are in wt %. The fields of rock compositions incorporate data from (Leonov and Rogozin, 2007), as well as our new unpublished analyses. The inset by the ($Na_2O + K_2O$) diagram shows the boundary of the diagram with respect to the entire compositional range.

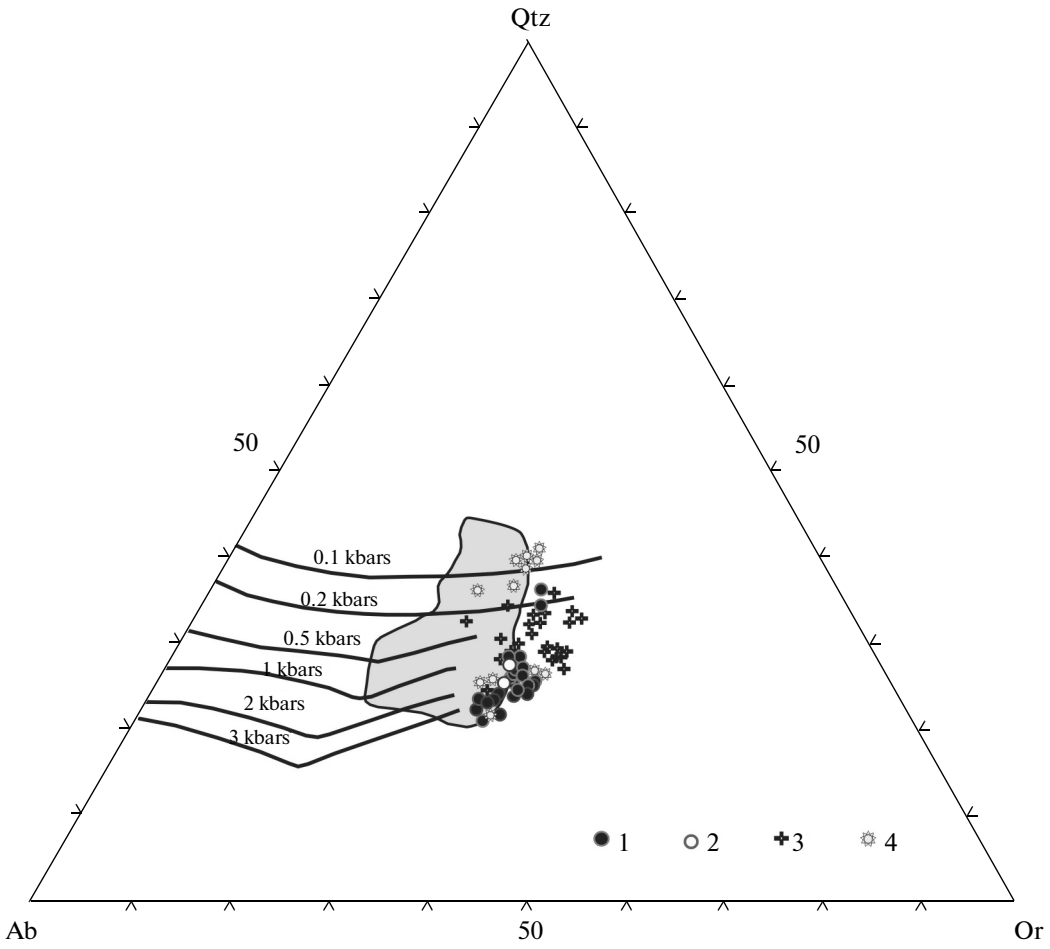

Fig. 6. Normative glass compositions in the Bannaya–Karymshina melt inclusions and rocks: (1) melt inclusions (MI) in quartz of precaldera ignimbrites, (2) MIs in the quartz of postcaldera ignimbrites, (3) MIs in the quartz of extrusions that contain sanidine in their phenocrysts, (4) MIs in the Yashchik quartz where sanidine is not present in the phenocrysts. The contour line encloses the composition of rocks for the area of study. The lines are cotectic curves with different concentrations of water (Winter, 2001).

ysis points for MI glasses with respect to the experimental cotectic curves, the pressure in the magma chamber at the time of quartz crystallization varied from 1.5–3.5 kbars (corresponding to depths of 5–9 km) for MIs in the quartz of pyroclastic deposits up to 0.1–2 kbars (corresponding to depths of 0.3–6 km) for MIs in phenocrysts of extrusive features. A large scatter of values, occasionally within a single grain, provides evidence of crystallization (or pre-crystallization) of quartz phenocrysts at different depths in a magma chamber (chambers) or in conduits. The maximum depth of quartz crystallization (8–9 km, 2–3.5 kbars) is characteristic for early ignimbrites along Nachikinskii Brook. The composition of the MIs from the quartz of these ignimbrites is the closest to the bulk composition of the rocks. The points for intracaldera ignimbrites plot in the diagram within the cotectic curves that correspond to a pressure of 1.5–2 kbars.

The quartz phenocrysts in the extrusive features occurred in a wider range of pressures. The overwhelming part of the MIs in quartz phenocrysts that were sampled from sanidine-bearing rhyolite extrusions plot as a compact set of points within the cotectic curves that correspond to pressures of 0.5–2.2 kbars (1.5–6 km) and are the farthest from the normative bulk compositions. The broadest range of pressure (0.1–3.5 kbars) is characteristic for glass in the Yashchik MIs where no sanidine was detected among the phenocrysts. The earliest melt inclusions, the ones that evolved the least, are related to relict quartz phenocrysts that crystallized from primary ignimbrite-generating melts that penetrated the shallow magma chamber as the melt was rising from deeper zones of the magmatic system. The melt inclusions that plot in the region of low pressure (0.1–0.2 kbars) in the diagram were probably captured under shallow conditions at depths of approximately 1 km. This is shown

by similarities between the composition of MI silicate phase and the groundmass glasses. The MI glass compositions in the quartz of extrusion lavas have higher concentrations of K_2O compared with the bulk composition of the rocks (see Fig. 5).

We carried out thermodynamic calculations for high-silica large-volume rhyolite ignimbrites in the United States (e.g., the Bishop Tuff in California), whose composition is close to that of the Bannaya–Karymshina ignimbrites, to show that the sequence of crystallization for phenocryst minerals in rocks of this type is in strict correspondence with pressure under the conditions of fluid (aqueous) saturation (Gualda et al., 2012).

For example, at pressures of 250–350 MPa (2.5–3.5 kbars) sanidine was the first crystalline phase. It was followed by crystallization of quartz and then of plagioclase. At 175 MPa quartz is the first phase, the next are sanidine and plagioclase. At low pressures (100 MPa) plagioclase is the first crystalline phase to be followed by sanidine and quartz. When the concentration of water in a melt is lower, the temperature of separation of sanidine increases from 754°C at 7 wt % H_2O to 892°C at 2 wt % H_2O. Sanidine contains less Or minal (58%) at low pressures compared with that at high pressures (79%). This finds confirmation in our data as well. The sanidine of Middle Pliocene ignimbrites that were formed at high pressures is richer in the potassium component

($Or_{71–77}$) than is the case in extrusions ($Or_{55–68}$) (see Table 2). Nearly simultaneous crystallization of sanidine and plagioclase as solid inclusions was only detected in few extrusions. An analysis of the Ab-Qtz-Or diagram shows that the compositions of melt inclusions do not invariably agree with the bulk compositions and differ in having more of the Or component.

Our results from the study of melt inclusions in quartz suggest the existence of an upper crustal magma chamber or chambers in the interior of the Bannaya-Karymshina area that contained subalkaline acid melts during 4 Ma (Leonov et al., 2013) and, at the lowest, the occurrence of a three-phase crystallization (or pre-crystallization) of quartz phenocrysts. The identification of three groups of primary glass-containing melt inclusions that were conserved in quartz phenocrysts in extrusions and which had different compositions suggests that the primary melts underwent changes during different phases in the evolution of the area and were erupted to make pyroclastic deposits and extrusive domes. The glasses in melt inclusions have trachyrhyodacitic and trachyrhyolitic compositions (the second group). They were found in corroded quartz phenocrysts in all rocks (samples) of different ages under study and obviously characterize melts from a deeper magma chamber (about 7–9 km). It is with these melt inclusions that one finds associated "moustaches" consisting of cracks, which indicate loss of sealing during the ascent of the melt that contained quartz phenocrysts to higher crustal levels. The movement of melt into volumes of lower pressures resulted in previously separated quartz crystals starting to be dissolved, while the melt inclusions experienced decrepitation under conditions in which internal pressure exceeded the external pressure by a value that was above the strength of the host mineral. Calculations show (Tait, 1992) that the limiting stress for inclusions of 20–30 μm at which brittle deformation starts in the quartz phenocryst is 2.0–2.5 kbars. For larger inclusions the cracks around a melt inclusion form when the pressure difference between inside and outside values is below 4 kbars. The presence of accessory manganese clinopyroxene and sphene (see Fig. 4) may indicate a relatively low amount of water in the melt. The observed deficit of sums of the components that was detected by microprobe analysis of glass in melt inclusions suggests that the concentration of H_2O in these varied in the range 1.4–2.6 wt %. Microcrystalline solid inclusions of clinopyroxene with rhodonite minal (4–10 wt % MnO) that were detected in melt inclusions in the quartz phenocrysts of older ignimbrites may provide evidence of possible assimilation of the clay-carbonate rocks in the basement of the structure by the melt. According to Deer et al. (1962), manganese clinopyroxenes (hedenbergite or ferrosillite) are characteristic for skarns that form in contact zones of intrusions and carbonate-bearing rocks. Grains that have not experienced complete dissolution contained within themselves those melt inclusions that were originally captured and that recovered their shapes under favorable conditions. Pre-crystallization can produce capture and conservation of both microportions of a farther evolved melt and of microcrystalline phases. The appearance in outer zones of some quartz phenocrysts of glass-containing melt inclusions of trachyrhyolite compositions and solid biotite inclusions provides evidence both of further crystallization in a farther evolved melt and of increasing role of volatile components in them, primarily water (the deficit of the sums reaches 5 wt %).

Sanidine is absent from among phenocrysts in Eopleistocene ignimbrites (the Karymshina caldera), and this indicates changes in the physico-chemical conditions of crystallization, pressure in the first place (Gualda et al., 2012). This may be due to movement of the melt to higher crustal levels and to decreasing temperature, as well as to effects due to melt assimilation and mixing.

When the caldera collapsed after ignimbrite discharge, the residual acid melts were squeezed toward upper crustal horizons along a ring fault. They probably formed a series of small magma chambers at differ-

ent depths that were evolving over time and forming post-caldera extrusive bodies. The melt inclusions in the quartz of sanidine-containing rhyolites deviate the most from the bulk composition toward the orthoclase component. Considering the zonality of the sanidine phenocrysts in extrusive features, one can hypothesize that this is due to emplacement into the base of the magma chamber of deeper, barium-rich melts and to variations in steam pressure during these injections.

All these hypotheses require additional proof and thermodynamic calculations to be carried out in the future.

ACKNOWLEDGMENTS

This work was supported by the "Far East" Program for the projects 15-1-2-031 and by the Russian Foundation for Basic Research, project no. 14-05-31319.

REFERENCES

Anikin, V.V. and Miller, E.L., The evolution of calc-alkaline magmas in the Sea-of-Okhotsk–Chukchi volcanogenic belt, *Petrologiya*, 2011, vol. 10, no. 1, pp. 249–290.

Bakumenko, I.T., Bazarova, T.Yu., and Panina, L.I., *Vklyucheniya silikatnykh i nesilikatnykh rasplavov v mineralakh* (Inclusions of Silicate and Nonsilicate Melts in Minerals), Moscow: Nauka, 1978, pp. 29–34.

Churikova, T.G., Verner, G., Mironov, N., et al., The variation in fluid composition across the Kamchatka island arc, in *Materialy IV mezhd. soveshchaniya po protsessam v zonakh subduktsii Yaponskoi, Kurilo-Kamchatskoi i Aleutskoi ostrovnykh dug "Vzaimosvyaz' mezhdu tektonikoi, seismichnost'yu, magmaobrazovaniem i izverzheniyami vulkanov v vulkanicheskikh dugakh"* (Proc. IV Intern. conf. on Processes in Subduction Zones of the Japanese, Kuril–Kamchatka, and Aleutian island arcs "Interrelationships among Tectonics, Seismicity, Magma Generation, and Volcanic Eruptions at Volcanic Island Arcs"), August 21–27, 2004, Petropavlovsk-Kamchatskii: IViS DVO RAN, 2004, pp. 119–120.

Deer, W.A., Howie, R.A., and Zussman, J., *Rock-Forming Minerals*, vol. 2, London: Longman, 1962.

Ehlers, E.G., *The Interpretation of Geological Phase Diagrams*, San Francisco: W. H. Freeman and Co., 1972.

Ermakov, N.P. and Dolgov, Yu.A., *Termobarogeokhimiya* (Thermal Barogeochemistry), Moscow: Nedra, 1979.

Gualdal, G.A., Ghiorso, M.S., Lemon, S.R., and Carley, T.I., Rhyolite-MELTS: Modified calibration of MELTS optimized for silica-rich, fluid-bearing magmatic systems, *J. Petrology*, 2012, vol. 53, no. 5, pp. 875–890.

Leonov, V.L. and Rogozin, A.N., Karymshina, a giant supervolcano caldera in Kamchatka: Boundaries, structure, volume of pyroclastics, *J. Volcanol. Seismol.*, 2007, vol. 1, no. 5, pp. 296–309.

Leonov, V.L., Bindeman, I.N., and Rogozin, A.N., New data on the volcanism that preceded the supereruption and generation of the Karymshina caldera, southern Kamchatka, in *Materialy konferentsii, posvyashchennoi Dnyu vulkanologa "Vulkanizm i svyazannye s nim protsessy"*(Proc. conf. devoted to Volcanologist's Day: "Volcanism and Related Processes"), March 28–29, Petropavlovsk-Kamchatskii: IViS DVO RAN, 2012, p. 56–63.

Leonov, V.L., Bindeman, I.N., Rogozin, A.N., and Anikin, L.P., New datings of volcanic rocks due to large-volume explosive eruptions in southern Kamchatka, in *Materialy konferentsii, posvyashchennoi Dnyu vulkanologa "Vulkanizm i svyazannye s nim protsessy"* (Proc.conf. devoted to Volcanologist's Day: "Volcanism and Related Processes"), March 28–29, 2013, Petropavlovsk-Kamchatskii: IViS DVO RAN, 2013, p. 33–34.

Mason, B.G., Pyle, D.M., and Oppenheimer, C., The size and frequency of the largest explosive eruptions on Earth, *Bull. Volcanology*, 2004, vol. 66, pp. 735–748.

Naumov, V.B., Tolstykh, M.L., Grib, E.N., et al., Chemical composition, volatile components and admixture elements in melts of Karymskii Volcanic Center (Kamchatka) and Golovnin Volcano (Kunashir Island) based on studies of inclusions in minerals, *Petrologiya*, 2008, vol. 16, no. 1, pp. 3–20.

Petrograficheskii kodeks. Magmaticheskie, metamorficheskie, metasomaticheskie, impaktnye obrazovaniya (Petrographic Code. Igneous, Metamorphic, Metasomatic, and Impact Formations), 2nd Edition, revised and supplemented, St. Petersburg: VSEGEI, 1995.

Poccerillo, A. and Taylor, S.R., Geochemistry of Eocene calc-alkaline volcanic rocks from the Kastomonu area, Northern Turkey, *Contrib. Mineral. Petrol.*, 1976, vol. 58, no. 1, pp. 63–81.

Sharkov, E.V., *Formirovanie rassloennykh intruzivov i svyazannogo s nimi orudeneniya* (The Formation of Stratified Intrusions and the Generation of Related Mineralization), Moscow: Nauchnyi Mir, 2006.

Shinkarev, N.F., *Fiziko-khimicheskaya petrologiya izverzhennykh porod* (Physico-Chemical Petrology of Igneous Rocks), Leningrad: Nedra, 1970.

Tait, S., Selective preservation of melt inclusions in igneous phenocrysts, *Amer. Mineral.*, 1992, vol. 77, pp. 146–154.

Winter, J.D., *An Introduction to Igneous and Metamorphic Petrology*, Englewood Cliffs, New Jersey: Prentice Hall, 2001.

Translated by A. Petrosyan